Cell Reports, Volume *43*

Supplemental information

An extended wave of global mRNA deadenylation sets up a switch in translation regulation across the mammalian oocyte-to-embryo transition

Katherine Lee, Kyucheol Cho, Robert Morey, and Heidi Cook-Andersen

Cell Reports, Volume ■ ■

Supplemental information

An extended wave of global mRNA deadenylation sets up a switch in translation regulation across the mammalian oocyte-to-embryo transition

Katherine Lee, Kyucheol Cho, Robert Morey, and Heidi Cook-Andersen

Supplementary Materials for

An extended wave of global mRNA deadenylation sets up a switch in translation regulation across the mammalian oocyte-to-embryo transition

Katherine Lee[2], Kyucheol Cho[1], Robert Morey[3], and Heidi Cook-Andersen[1,2,4]

[4]Correspondence: Heidi Cook-Andersen (hcookandersen@health.ucsd.edu)

This PDF file includes:

Figs. S1 to S10

Other Supplementary Materials for this manuscript include the following:

Data S1 to S4:
Data S1_Sequencing_Tail_Lengths_TranscriptIDs_Stability_MEG.xlsx
Data S2_GO_Analyses.xlsx
Data S3_Isoform_Tail_Length_Regulation.xlsx
Data S4_RBP_3'UTR_Motif_Enrichment.xlsx

Figure S1

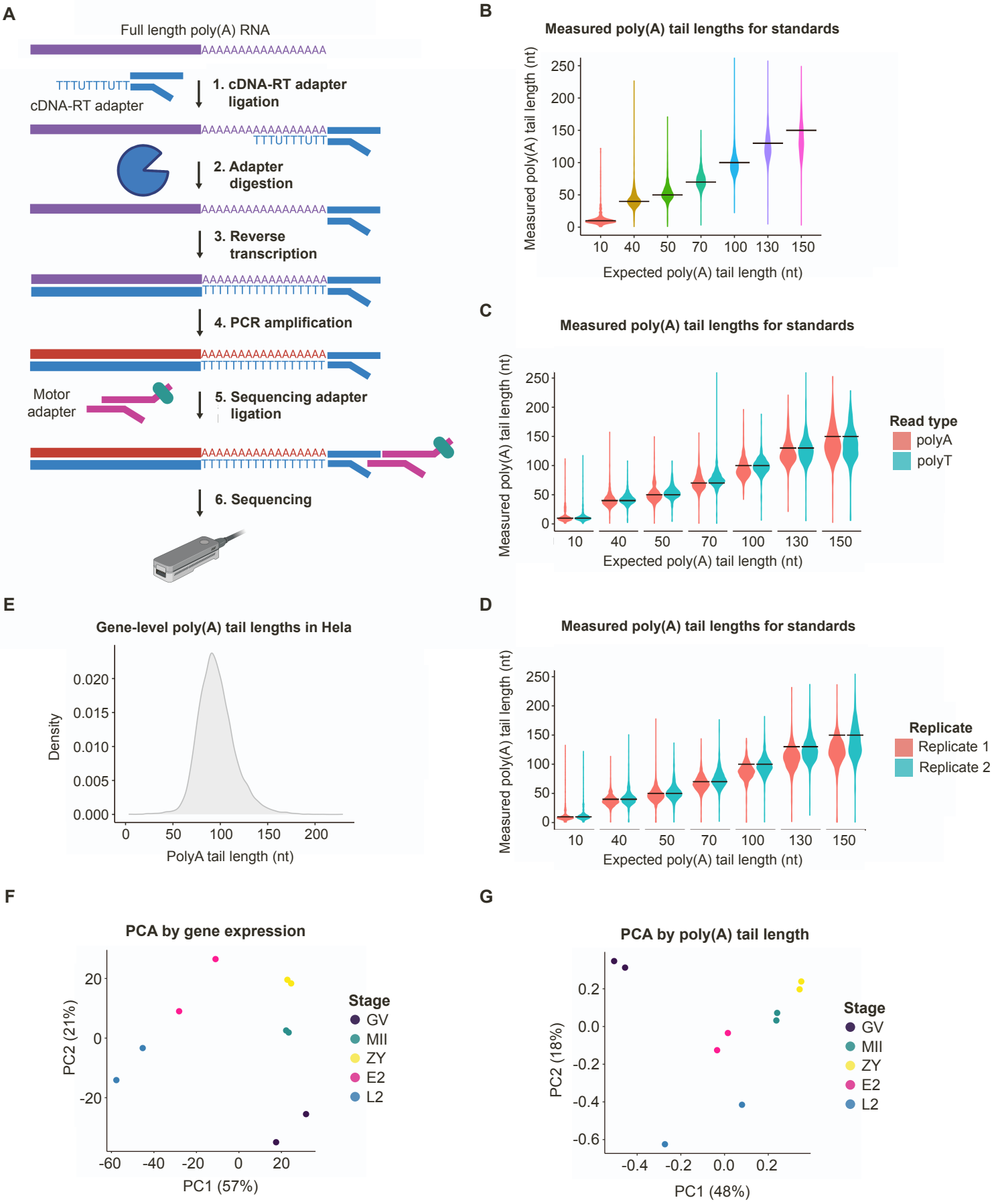
A
Full length poly(A) RNA
AAAAAAAAAAAAAAAA
TTTUTTTUTT
cDNA-RT adapter
1. cDNA-RT adapter ligation
2. Adapter digestion
3. Reverse transcription
4. PCR amplification
Motor adapter
5. Sequencing adapter ligation
6. Sequencing
B
Measured poly(A) tail lengths for standards
Measured poly(A) tail length (nt)
Expected poly(A) tail length (nt)
C
Measured poly(A) tail lengths for standards
Read type
polyA
polyT
D
Measured poly(A) tail lengths for standards
Replicate
Replicate 1
Replicate 2
E
Gene-level poly(A) tail lengths in Hela
Density
PolyA tail length (nt)
F
PCA by gene expression
PC1 (57%)
PC2 (21%)
Stage
GV
MII
ZY
E2
L2
G
PCA by poly(A) tail length
PC1 (48%)
PC2 (18%)
Stage
GV
MII
ZY
E2
L2

Figure S1. Nanopore PCR-cDNA sequencing accurately and reproducibly measures poly(A) tail lengths, Related to Figure 1. (A) Schematic of Nanopore PCR-cDNA sequencing. (B) Measured tail lengths for 7 standards of different poly(A) tail lengths. (C-D) Same as (B) but separated by read type (C) or replicate (D). For (B-D), horizontal lines indicate expected poly(A) tail lengths for each standard. (E) Global distribution of gene-level mean poly(A) tail lengths in Hela. Only genes with ≥10 polyadenylated reads were included. (F) PCA clustering of developmental stages and biological replicates by gene expression. (G) PCA clustering of developmental stages and biological replicates by poly(A) tail length.

Figure S2

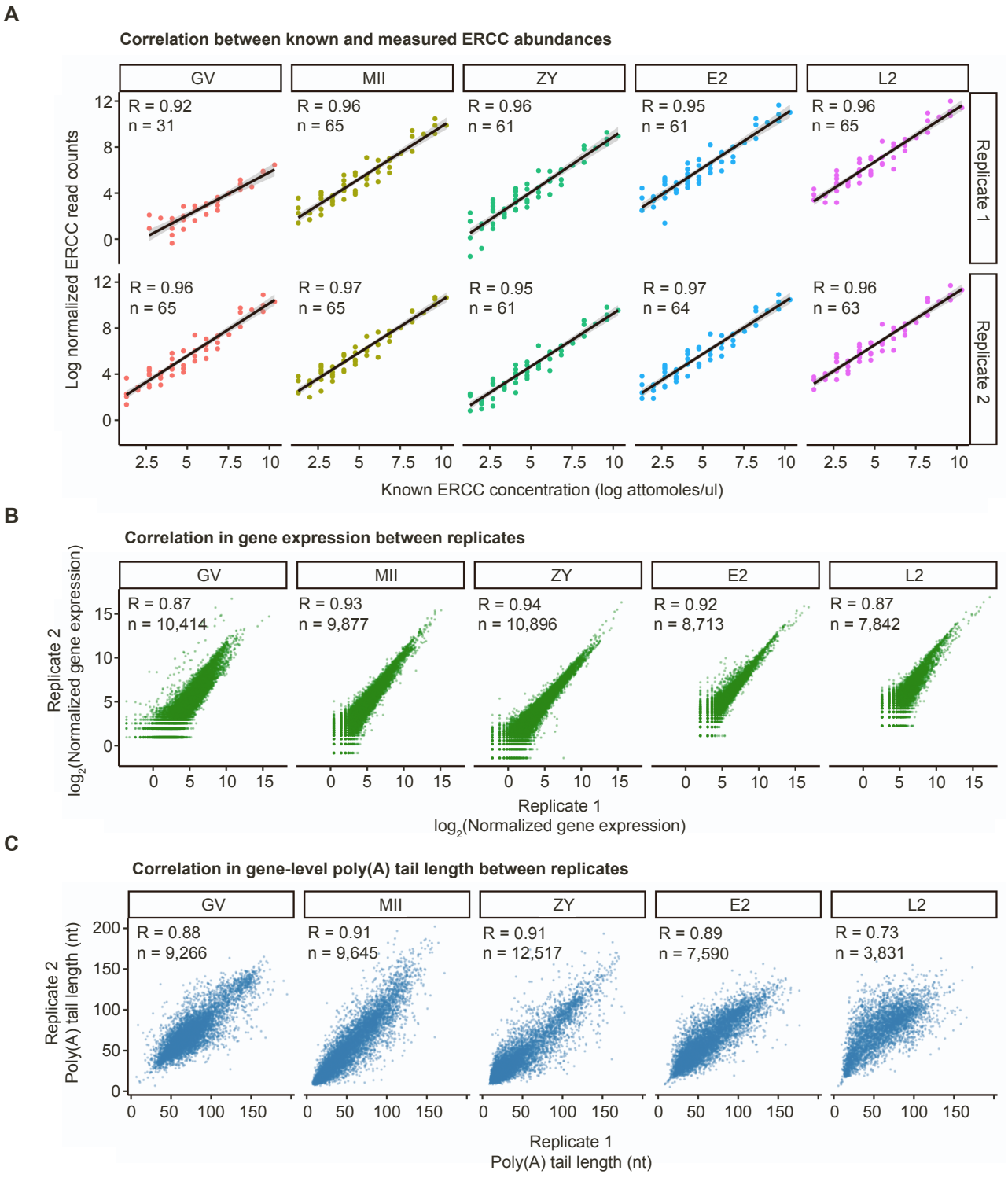
A
Correlation between known and measured ERCC abundances
GV
MII
ZY
E2
L2
R = 0.92
n = 31
R = 0.96
n = 65
R = 0.96
n = 61
R = 0.95
n = 61
R = 0.96
n = 65
R = 0.96
n = 65
R = 0.97
n = 65
R = 0.95
n = 61
R = 0.97
n = 64
R = 0.96
n = 63
Replicate 1
Replicate 2
Log normalized ERCC read counts
Known ERCC concentration (log attomoles/ul)
B
Correlation in gene expression between replicates
R = 0.87
n = 10,414
R = 0.93
n = 9,877
R = 0.94
n = 10,896
R = 0.92
n = 8,713
R = 0.87
n = 7,842
log2(Normalized gene expression)
Replicate 1
log2(Normalized gene expression)
C
Correlation in gene-level poly(A) tail length between replicates
R = 0.88
n = 9,266
R = 0.91
n = 9,645
R = 0.91
n = 12,517
R = 0.89
n = 7,590
R = 0.73
n = 3,831
Poly(A) tail length (nt)
Replicate 1
Poly(A) tail length (nt)

Figure S2. Nanopore PCR-cDNA sequencing reproducibly captures poly(A) tail lengths and gene expression profiles across the OET, Related to Figure 1. (A) Correlation between known and measured abundances for ERCC standards. (B) Correlation in gene expression between biological replicates. (C) Correlation in gene-level poly(A) tail length between biological replicates. Only genes with ≥20 polyadenylated reads in each replicate are plotted. R, Pearson correlation coefficient; n, number of genes or ERCC standards.

Figure S3

A

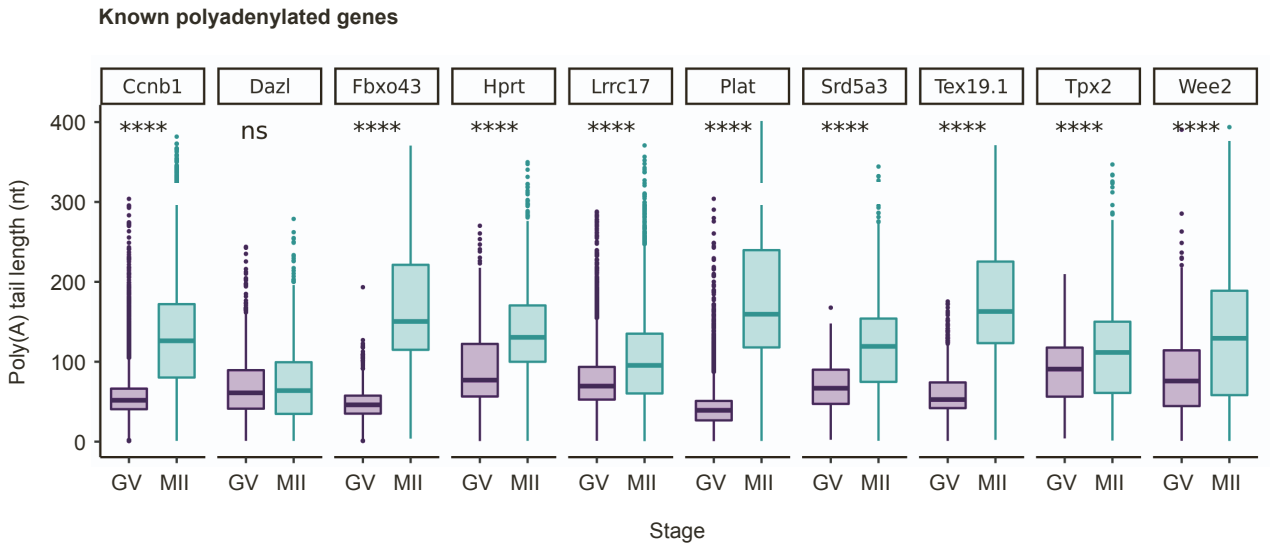
Known polyadenylated genes
Ccnb1
Dazl
Fbxo43
Hprt
Lrrc17
Plat
Srd5a3
Tex19.1
Tpx2
Wee2
****
ns
Poly(A) tail length (nt)
0
100
200
300
400
GV
MII
Stage

B

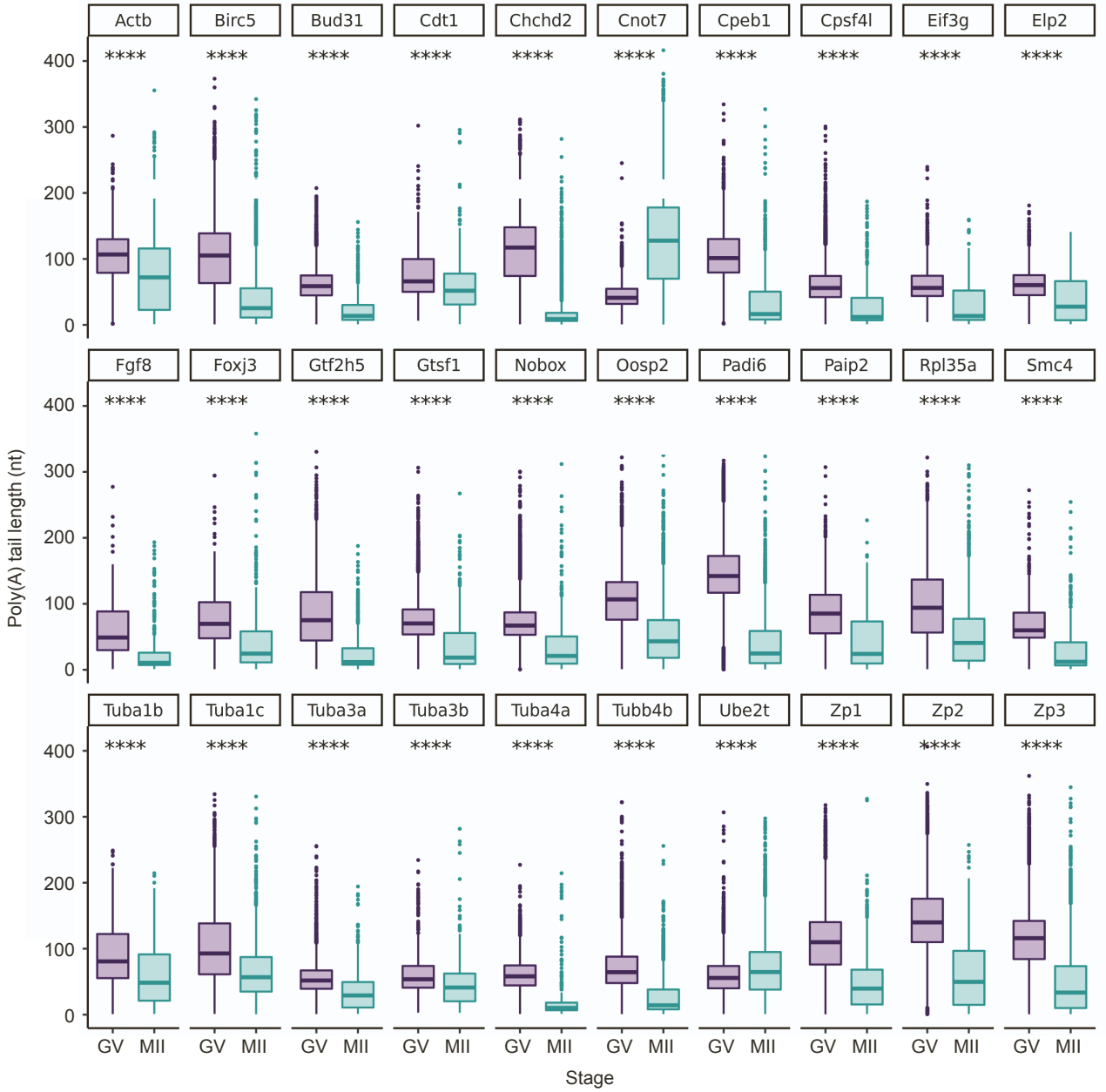
Known deadenylated genes
Actb
Birc5
Bud31
Cdt1
Chchd2
Cnot7
Cpeb1
Cpsf4l
Eif3g
Elp2
Fgf8
Foxj3
Gtf2h5
Gtsf1
Nobox
Oosp2
Padi6
Paip2
Rpl35a
Smc4
Tuba1b
Tuba1c
Tuba3a
Tuba3b
Tuba4a
Tubb4b
Ube2t
Zp1
Zp2
Zp3
****
Poly(A) tail length (nt)
0
100
200
300
400
GV
MII
Stage

Figure S3. Nanopore PCR-cDNA sequencing accurately captures known changes in poly(A) tail length for individual genes, Related to Figure 1. (A-B) Measured poly(A) tail lengths in GV and MII oocytes for all identified genes previously shown to be polyadenylated (A) or deadenylated (B) during oocyte maturation using an orthogonal method [1-15]. One-sided Wilcoxon tests shown ($^{****}p \leq 0.0001$). Two genes (Btg4 and Mos) were excluded for conflicting published tail length changes [3,7,16].

Figure S4

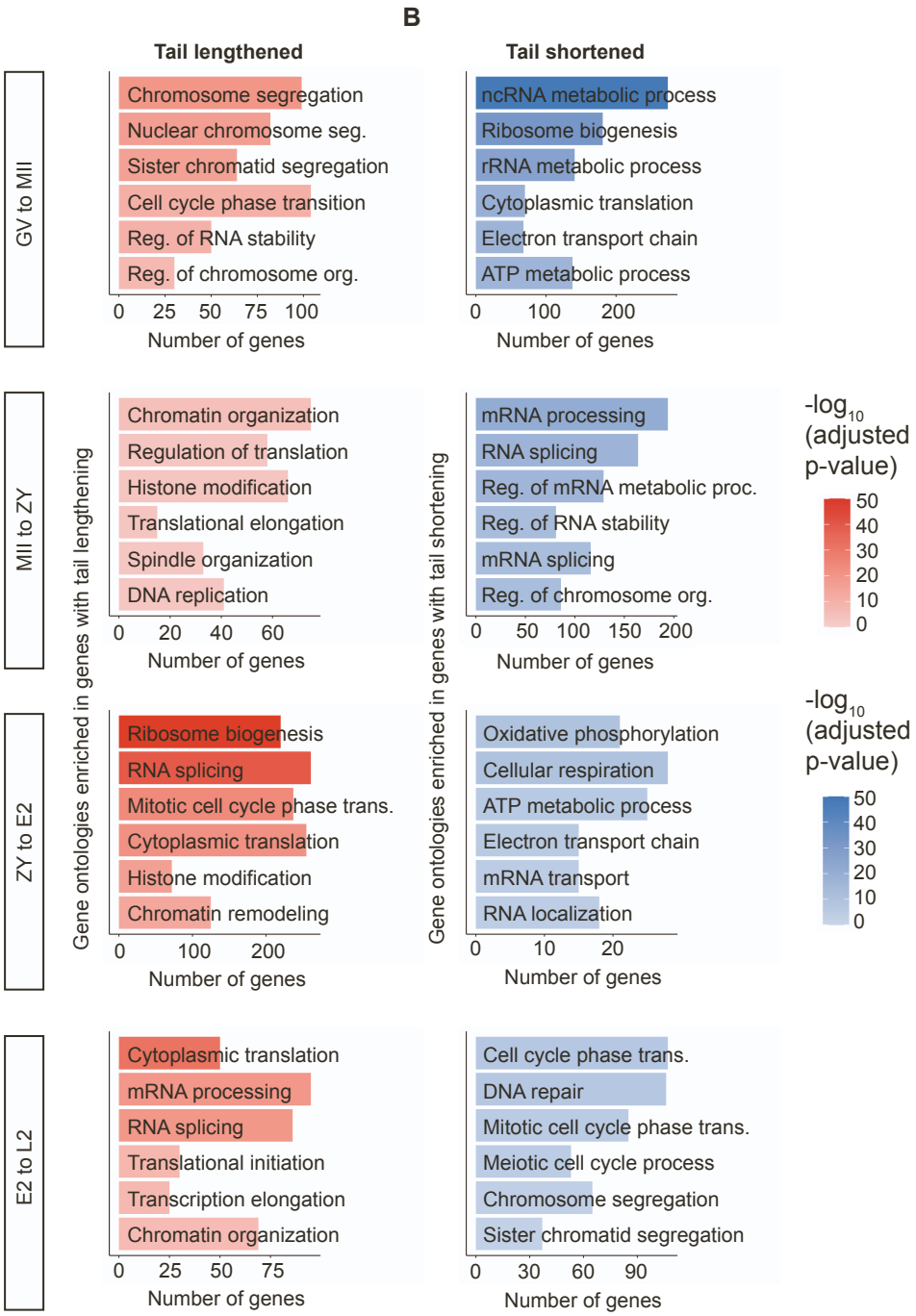
A
B
Tail lengthened
Tail shortened
GV to MII
MII to ZY
ZY to E2
E2 to L2
Gene ontologies enriched in genes with tail lengthening
Gene ontologies enriched in genes with tail shortening
Chromosome segregation
Nuclear chromosome seg.
Sister chromatid segregation
Cell cycle phase transition
Reg. of RNA stability
Reg. of chromosome org.
ncRNA metabolic process
Ribosome biogenesis
rRNA metabolic process
Cytoplasmic translation
Electron transport chain
ATP metabolic process
Chromatin organization
Regulation of translation
Histone modification
Translational elongation
Spindle organization
DNA replication
mRNA processing
RNA splicing
Reg. of mRNA metabolic proc.
Reg. of RNA stability
mRNA splicing
Reg. of chromosome org.
Ribosome biogenesis
RNA splicing
Mitotic cell cycle phase trans.
Cytoplasmic translation
Histone modification
Chromatin remodeling
Oxidative phosphorylation
Cellular respiration
ATP metabolic process
Electron transport chain
mRNA transport
RNA localization
Cytoplasmic translation
mRNA processing
RNA splicing
Translational initiation
Transcription elongation
Chromatin organization
Cell cycle phase trans.
DNA repair
Mitotic cell cycle phase trans.
Meiotic cell cycle process
Chromosome segregation
Sister chromatid segregation
Number of genes
-log10 (adjusted p-value)

Figure S4. Polyadenylated mRNAs at each stage are enriched for factors with stage-specific developmental roles, Related to Figure 1. Gene ontologies enriched in genes with significantly lengthened (red) (A) and shortened (blue) (B) tail lengths at each stage transition.

Figure S5

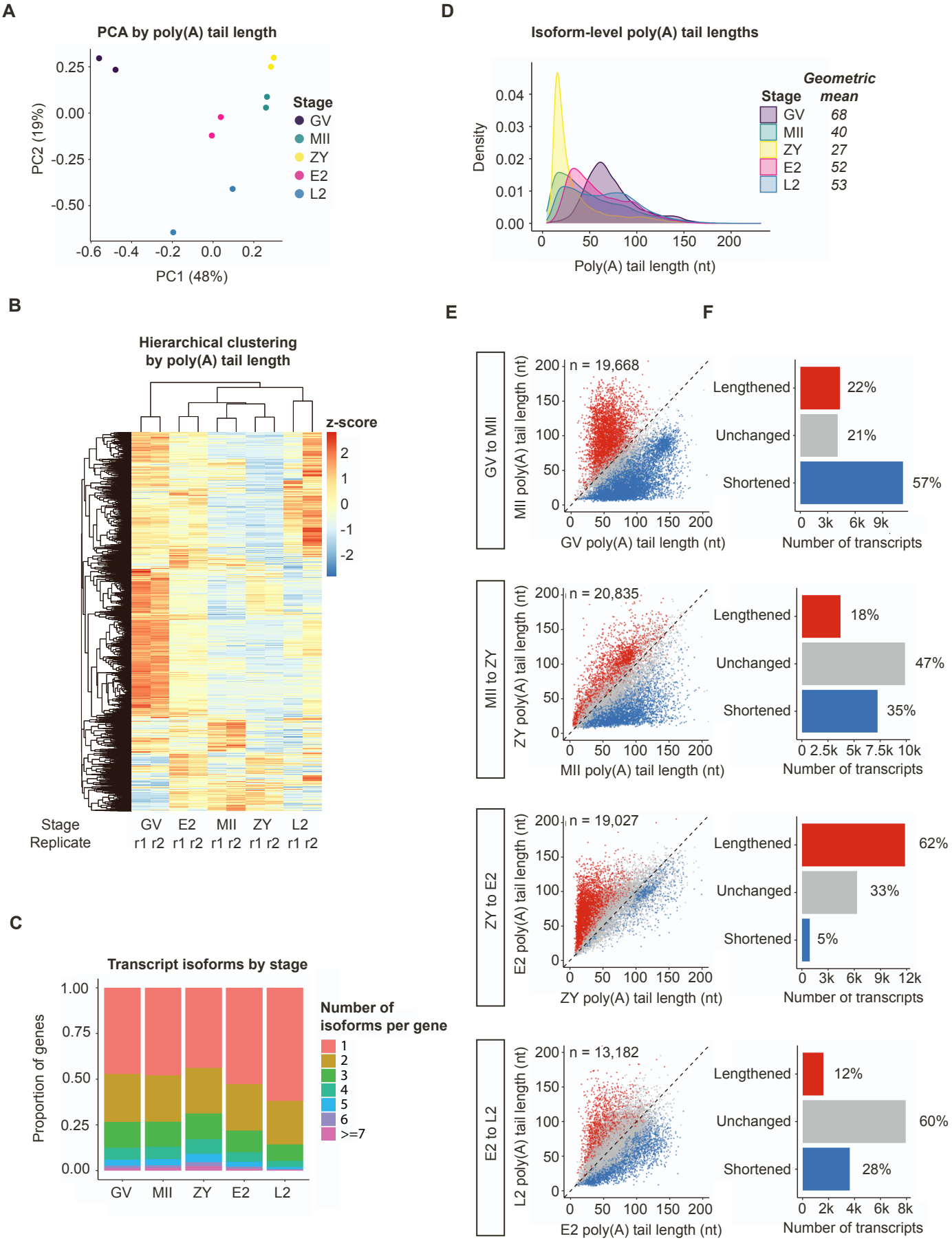
A
PCA by poly(A) tail length
PC2 (19%)
PC1 (48%)
Stage
GV
MII
ZY
E2
L2
B
Hierarchical clustering
by poly(A) tail length
z-score
Stage
Replicate
GV E2 MII ZY L2
r1 r2 r1 r2 r1 r2 r1 r2 r1 r2
C
Transcript isoforms by stage
Proportion of genes
Number of
isoforms per gene
GV MII ZY E2 L2
D
Isoform-level poly(A) tail lengths
Density
Poly(A) tail length (nt)
Geometric
mean
GV 68
MII 40
ZY 27
E2 52
L2 53
E
F
GV to MII
n = 19,668
MII poly(A) tail length (nt)
GV poly(A) tail length (nt)
Lengthened 22%
Unchanged 21%
Shortened 57%
Number of transcripts
MII to ZY
n = 20,835
ZY poly(A) tail length (nt)
MII poly(A) tail length (nt)
Lengthened 18%
Unchanged 47%
Shortened 35%
Number of transcripts
ZY to E2
n = 19,027
E2 poly(A) tail length (nt)
ZY poly(A) tail length (nt)
Lengthened 62%
Unchanged 33%
Shortened 5%
Number of transcripts
E2 to L2
n = 13,182
L2 poly(A) tail length (nt)
E2 poly(A) tail length (nt)
Lengthened 12%
Unchanged 60%
Shortened 28%
Number of transcripts

Figure S5. mRNA poly(A) tails are dynamically regulated at the isoform-level, Related to Figure 2. (A) PCA clustering of developmental stages and biological replicates by isoform-level poly(A) tail length. (B) Hierarchical clustering of stages and biological replicates by isoform-level poly(A) tail length. (C) Proportion of genes with different numbers of isoforms by stage. (D) Density plots showing global distributions of isoform-level mean poly(A) tail lengths at each stage. (E) Scatterplots showing mean poly(A) tail lengths for isoforms with significantly increased (lengthened, red), decreased (shortened, blue) or unchanged (gray) tail length at each stage transition (adj. $p < 0.05$, one-sided Wilcoxon test). (F) Number of genes in each category in (E).

Figure S6

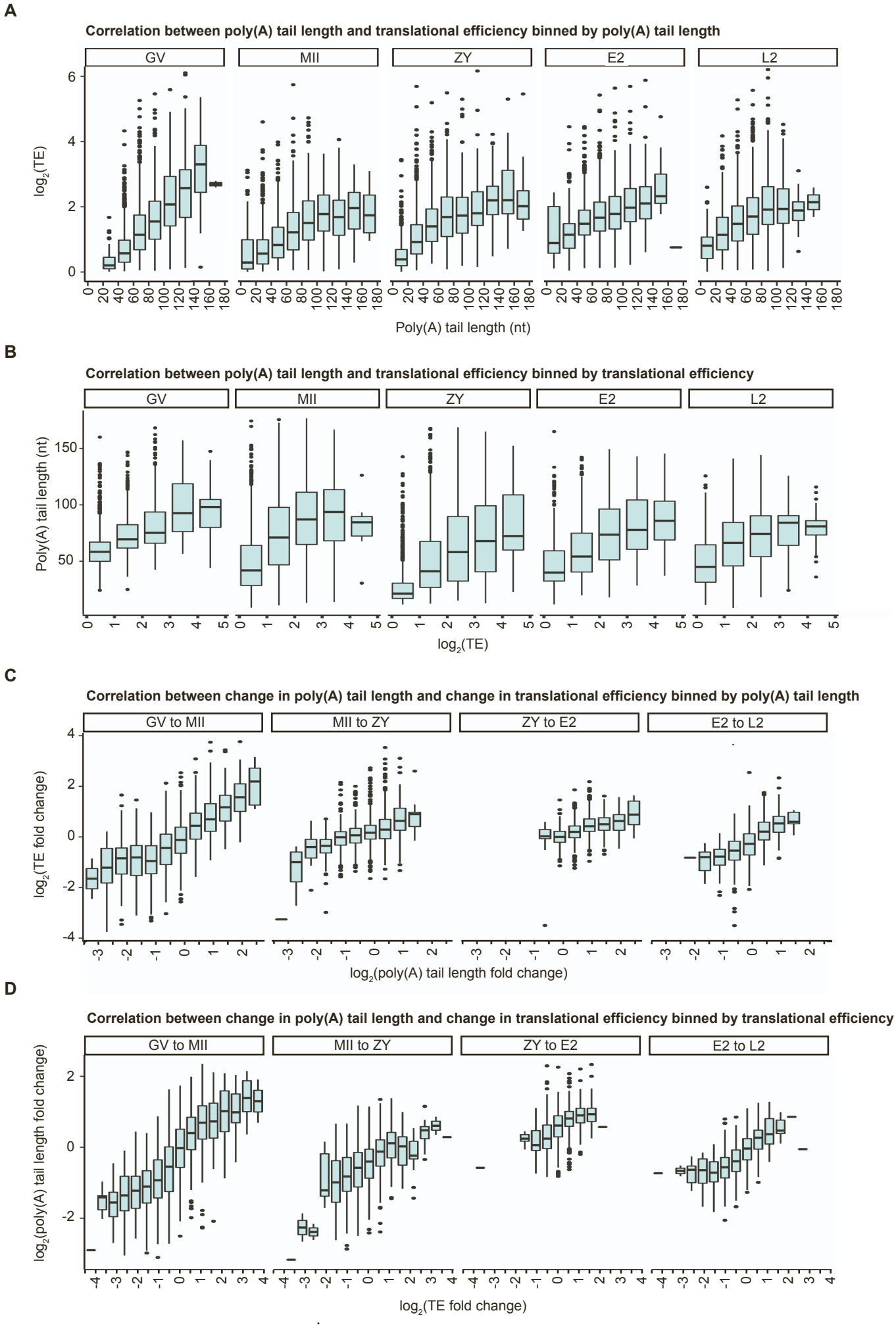
A
Correlation between poly(A) tail length and translational efficiency binned by poly(A) tail length
GV
MII
ZY
E2
L2
log2(TE)
Poly(A) tail length (nt)
B
Correlation between poly(A) tail length and translational efficiency binned by translational efficiency
Poly(A) tail length (nt)
log2(TE)
C
Correlation between change in poly(A) tail length and change in translational efficiency binned by poly(A) tail length
GV to MII
MII to ZY
ZY to E2
E2 to L2
log2(TE fold change)
log2(poly(A) tail length fold change)
D
Correlation between change in poly(A) tail length and change in translational efficiency binned by translational efficiency
log2(poly(A) tail length fold change)
log2(TE fold change)

Figure S6. Poly(A) tail length positively correlates with translational efficiency during OET, Related to Figure 4. (A) Translational efficiency of genes binned by poly(A) tail length at each stage. (B) Poly(A) length of genes binned by translational efficiency at each stage. (C) Change in translational efficiency of genes binned by change in poly(A) tail length between consecutive stages. (D) Change in poly(A) tail length of genes binned by change in translational efficiency between consecutive stages. TE, translational efficiency.

Figure S7

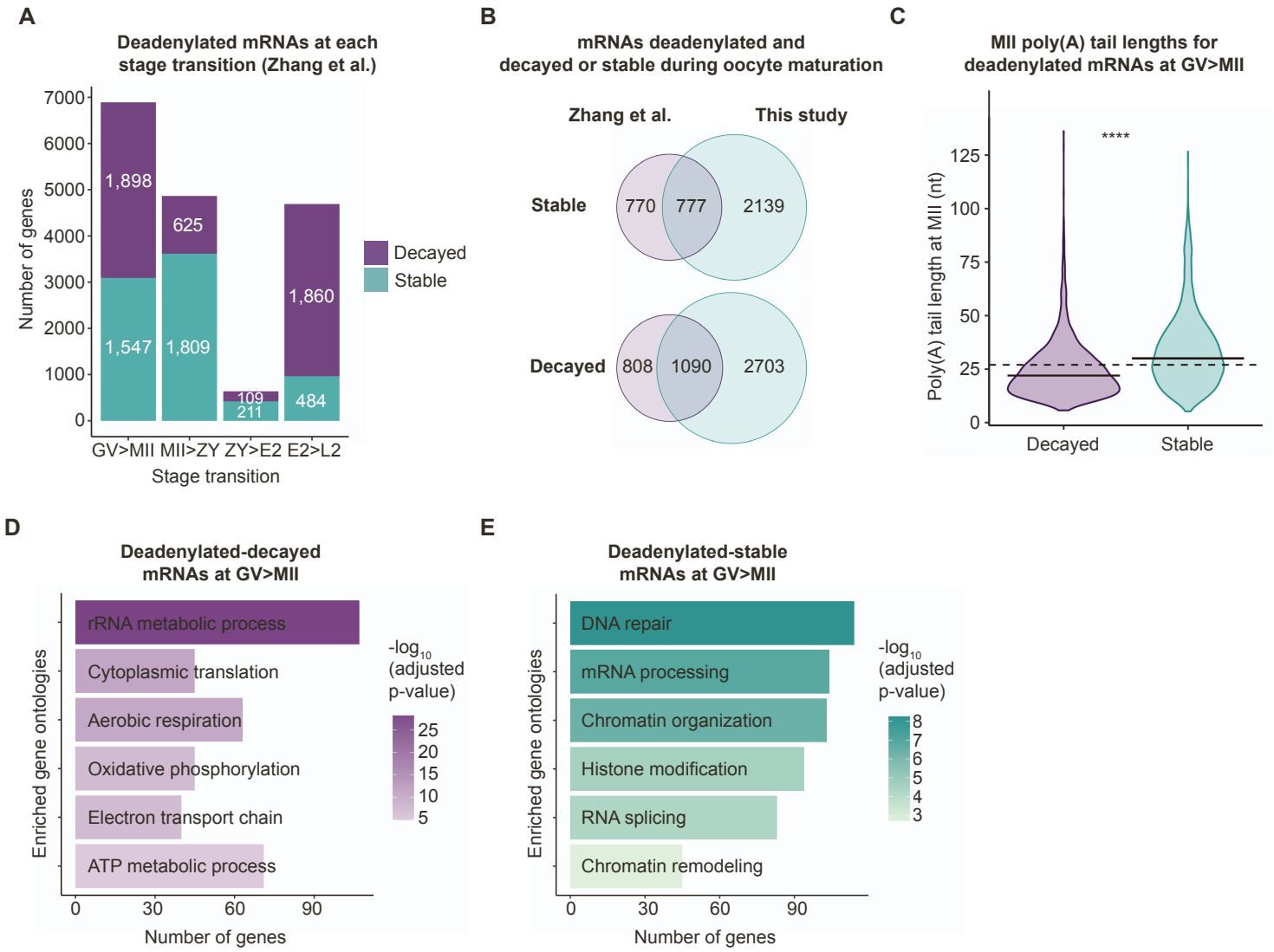
A
Deadenylated mRNAs at each stage transition (Zhang et al.)
Number of genes
7000
6000
5000
4000
3000
2000
1000
0
1,898
1,547
625
1,809
109
211
1,860
484
GV>MII
MII>ZY
ZY>E2
E2>L2
Stage transition
Decayed
Stable
B
mRNAs deadenylated and decayed or stable during oocyte maturation
Zhang et al.
This study
Stable
770
777
2139
Decayed
808
1090
2703
C
MII poly(A) tail lengths for deadenylated mRNAs at GV>MII
Poly(A) tail length at MII (nt)
125
100
75
50
25
0
****
Decayed
Stable
D
Deadenylated-decayed mRNAs at GV>MII
Enriched gene ontologies
rRNA metabolic process
Cytoplasmic translation
Aerobic respiration
Oxidative phosphorylation
Electron transport chain
ATP metabolic process
0
30
60
90
Number of genes
-log10 (adjusted p-value)
25
20
15
10
5
E
Deadenylated-stable mRNAs at GV>MII
Enriched gene ontologies
DNA repair
mRNA processing
Chromatin organization
Histone modification
RNA splicing
Chromatin remodeling
0
30
60
90
Number of genes
-log10 (adjusted p-value)
8
7
6
5
4
3

Figure S7. Deadenylated maternal mRNAs coupled and uncoupled from mRNA decay, Related to Figure 5. (A) Number of deadenylated-decayed (purple) or -stable (teal) genes at each stage transition using RNA abundances measured in Zhang et al. [17] integrated with poly(A) tail lengths measured in this dataset. (B) Venn diagrams demonstrating overlap of these genes with those identified using RNA abundances and poly(A) tail lengths measured in this study. (C) Poly(A) tail lengths at the MII stage of genes deadenylated-decayed (purple) or -stable (teal) during oocyte maturation. Solid horizontal lines indicate geometric means. Dashed horizontal line at indicates predicted PABP footprint of 27 nucleotides. Two-sided Wilcoxon test shown ($^{****}p \leq 0.0001$). (D-E) Gene ontologies enriched in genes deadenylated-decayed (D) or -stable (E) during oocyte maturation.

Figure S8

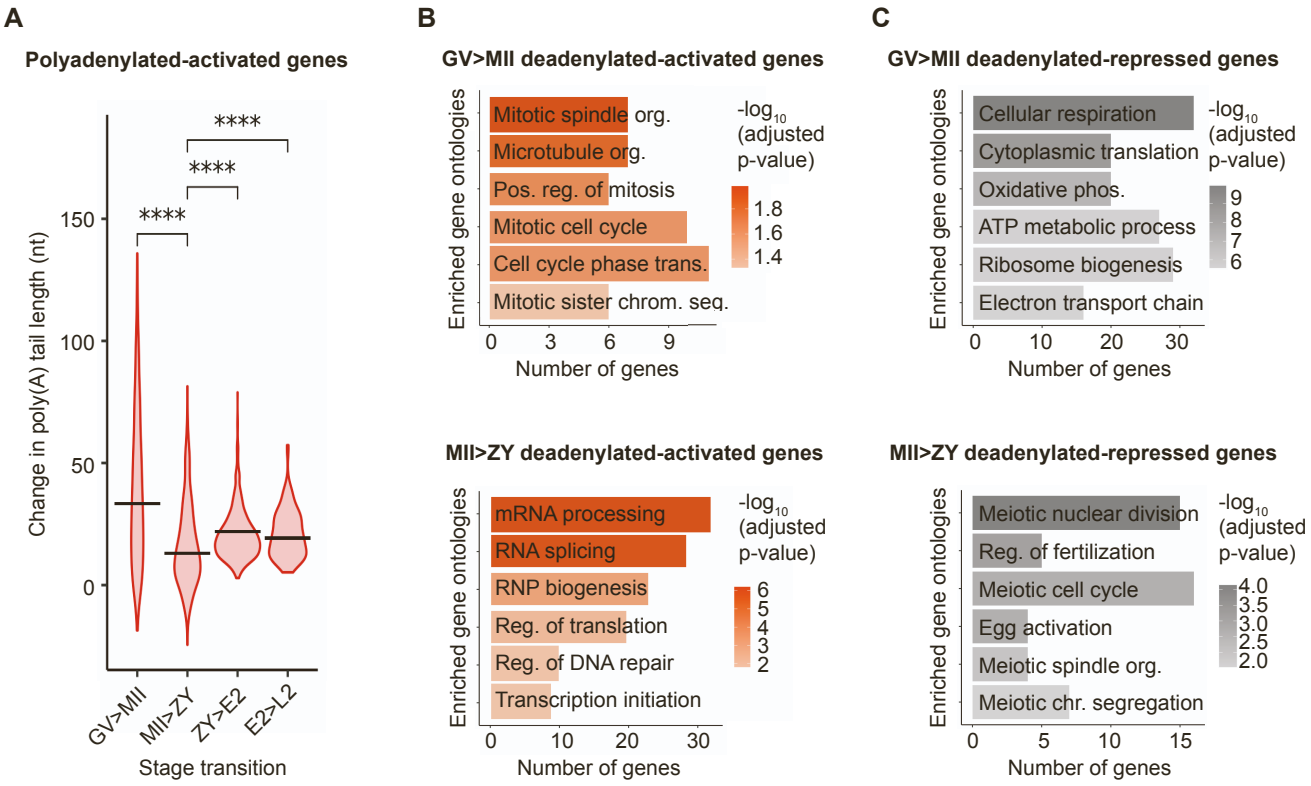
A
Polyadenylated-activated genes
Change in poly(A) tail length (nt)
150
100
50
0
****
****
****
GV>MII
MII>ZY
ZY>E2
E2>L2
Stage transition
B
GV>MII deadenylated-activated genes
Enriched gene ontologies
Mitotic spindle org.
Microtubule org.
Pos. reg. of mitosis
Mitotic cell cycle
Cell cycle phase trans.
Mitotic sister chrom. seg.
0 3 6 9
Number of genes
-log10 (adjusted p-value)
1.8
1.6
1.4
MII>ZY deadenylated-activated genes
Enriched gene ontologies
mRNA processing
RNA splicing
RNP biogenesis
Reg. of translation
Reg. of DNA repair
Transcription initiation
0 10 20 30
Number of genes
-log10 (adjusted p-value)
6
5
4
3
2
C
GV>MII deadenylated-repressed genes
Enriched gene ontologies
Cellular respiration
Cytoplasmic translation
Oxidative phos.
ATP metabolic process
Ribosome biogenesis
Electron transport chain
0 10 20 30
Number of genes
-log10 (adjusted p-value)
9
8
7
6
MII>ZY deadenylated-repressed genes
Enriched gene ontologies
Meiotic nuclear division
Reg. of fertilization
Meiotic cell cycle
Egg activation
Meiotic spindle org.
Meiotic chr. segregation
0 5 10 15
Number of genes
-log10 (adjusted p-value)
4.0
3.5
3.0
2.5
2.0

Figure S8. Genes translationally activated by resistance to global deadenylation play developmentally important roles, Related to Figure 6. (A) Change in poly(A) tail length for polyadenylated genes with increased translational efficiency at each stage transition. Horizontal lines indicate arithmetic means. Pairwise two-sided Wilcoxon tests shown for all stage transitions compared to MII>ZY ($^{****}p \leq 0.0001$). (B) Gene ontologies enriched in genes deadenylated-activated during oocyte maturation (GV>MII, top) or fertilization (MII>ZY, bottom). (C) Gene ontologies enriched in genes deadenylated-repressed during oocyte maturation (GV>MII, top) or fertilization (MII>ZY, bottom).

Figure S9

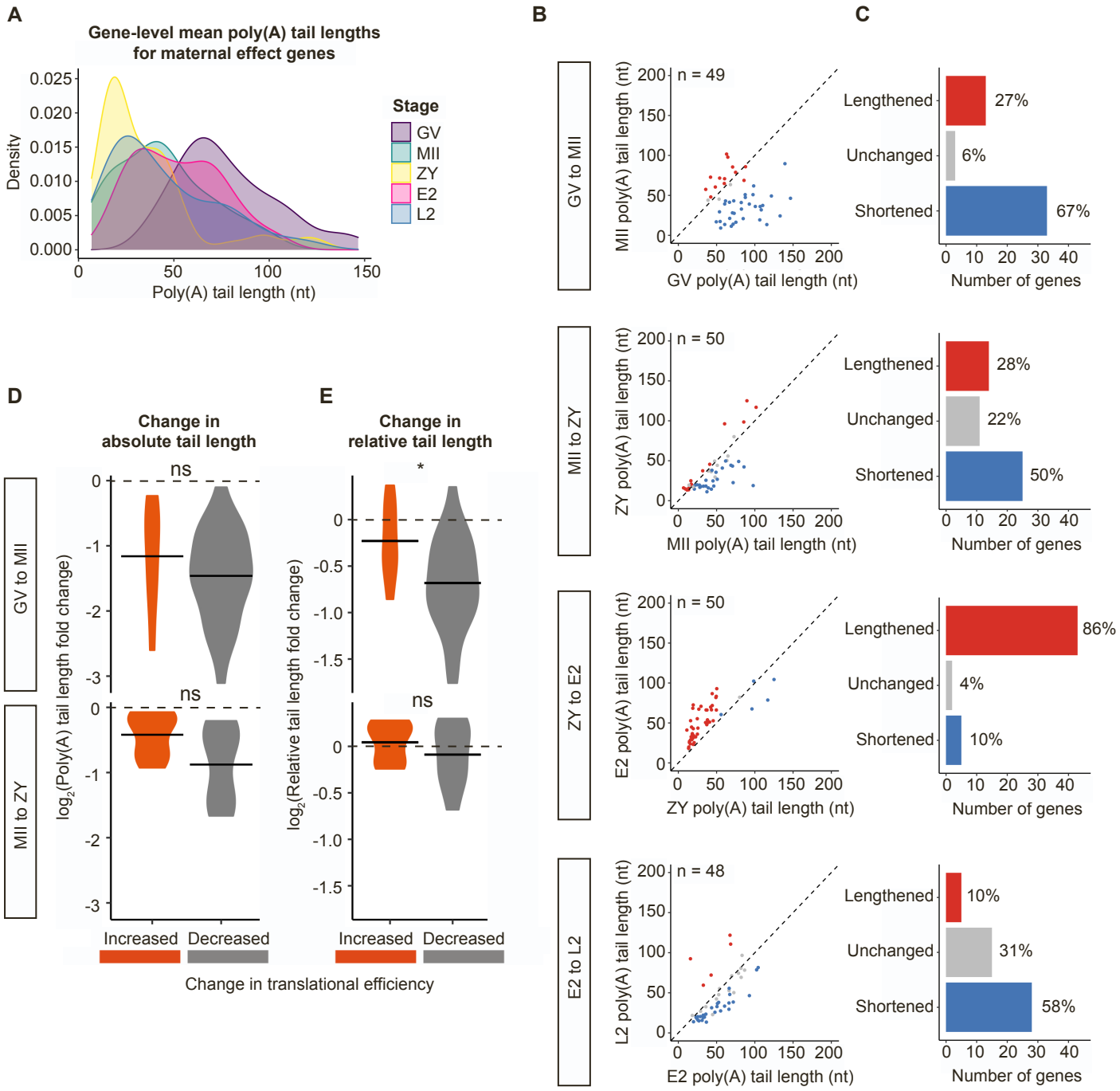
A
Gene-level mean poly(A) tail lengths for maternal effect genes
Density
Poly(A) tail length (nt)
Stage
GV
MII
ZY
E2
L2
B
C
GV to MII
MII to ZY
ZY to E2
E2 to L2
n = 49
n = 50
n = 50
n = 48
GV poly(A) tail length (nt)
MII poly(A) tail length (nt)
ZY poly(A) tail length (nt)
E2 poly(A) tail length (nt)
Lengthened
Unchanged
Shortened
27%
6%
67%
28%
22%
50%
86%
4%
10%
10%
31%
58%
Number of genes
D
Change in absolute tail length
log2(Poly(A) tail length fold change)
ns
E
Change in relative tail length
log2(Relative tail length fold change)
*
Increased
Decreased
Change in translational efficiency

Figure S9. Dynamic regulation of poly(A) tail length of maternal effect genes (MEGs), Related to Figure 7. (A) Density plots showing global distributions of gene-level mean poly(A) tail lengths at each stage for MEGs. (B) Scatterplots showing mean poly(A) tail lengths for MEGs with significantly increased (lengthened, red), decreased (shortened, blue) or unchanged (gray) tail lengths at each stage transition (adj. $p < 0.05$, one-sided Wilcoxon test). (C) Number of genes in each category in (B). (D-E) Log_2 fold change in absolute (D) or relative (E) tail length for deadenylated-activated (orange) or -repressed (gray) MEGs across each stage transition. Horizontal lines indicate arithmetic means. To include genes translationally activated or repressed despite no significant change in tail length, the adjusted p value cutoff for classifying genes as deadenylated was removed. Two-sided Wilcoxon tests are shown (ns, $p > 0.05$; $^{*}p \leq 0.05$).

Figure S10

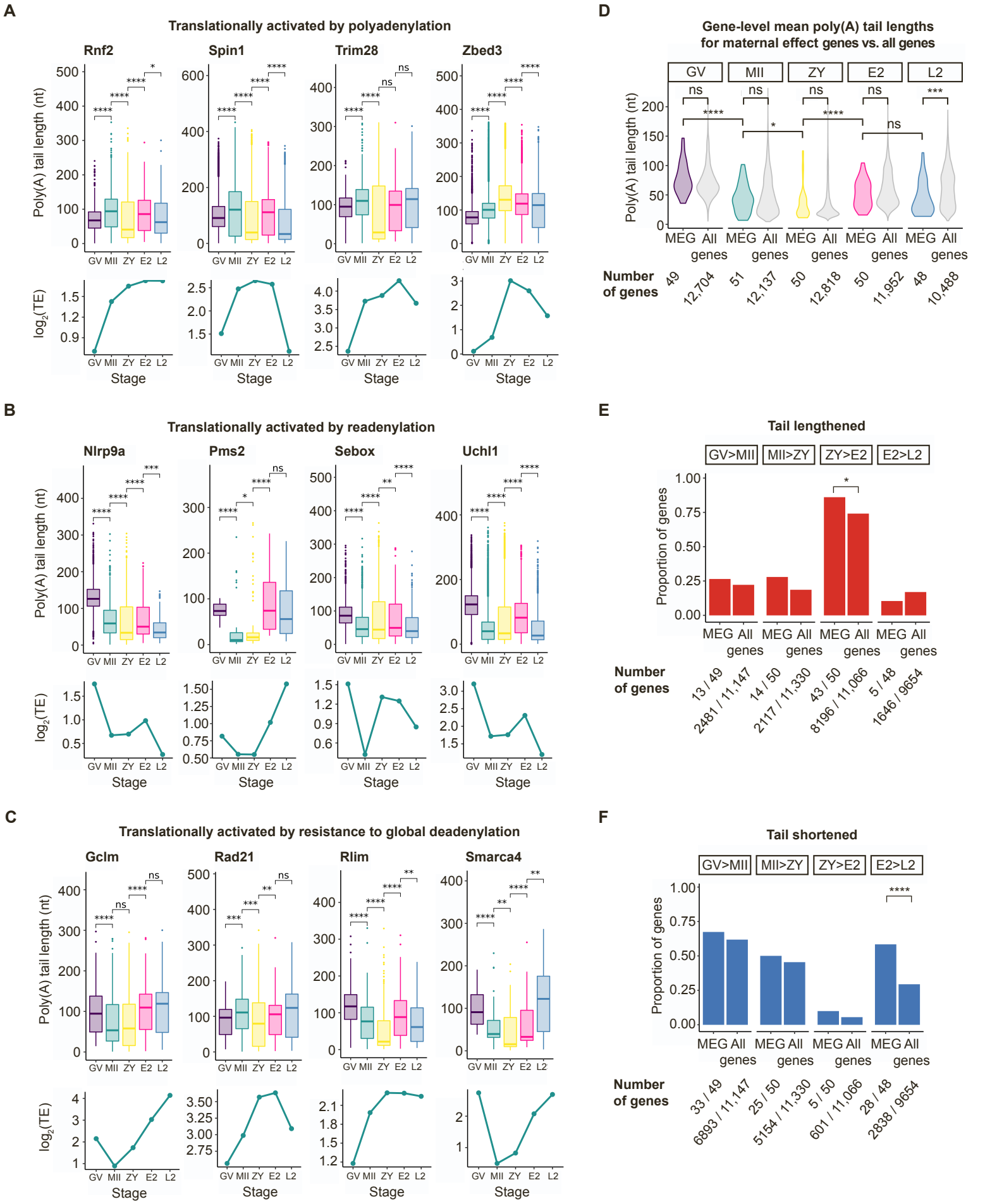
A
Translationally activated by polyadenylation
Rnf2
Spin1
Trim28
Zbed3
Poly(A) tail length (nt)
log2(TE)
GV MII ZY E2 L2
Stage
B
Translationally activated by readenylation
Nlrp9a
Pms2
Sebox
Uchl1
C
Translationally activated by resistance to global deadenylation
Gclm
Rad21
Rlim
Smarca4
D
Gene-level mean poly(A) tail lengths
for maternal effect genes vs. all genes
GV
MII
ZY
E2
L2
MEG
All genes
Number of genes
49
12,704
51
12,137
50
12,818
50
11,952
48
10,488
E
Tail lengthened
GV>MII
MII>ZY
ZY>E2
E2>L2
Proportion of genes
Number of genes
13 / 49
2481 / 11,147
14 / 50
2117 / 11,330
43 / 50
8196 / 11,066
5 / 48
1646 / 9654
F
Tail shortened
Number of genes
33 / 49
6893 / 11,147
25 / 50
5154 / 11,330
5 / 50
601 / 11,066
28 / 48
2838 / 9654

Figure S10. Additional examples of poly(A) tail and TE regulation of maternal effect genes, Related to Figure 7. (A-C) Poly(A) tail lengths (upper) and translational efficiencies (lower) of select maternal effect genes across the OET. Each box plot represents ≥ 20 polyadenylated reads. Pairwise two-sided Wilcoxon tests are shown (ns, $p > 0.05$; $^{*}p \leq 0.05$; $^{**}p \leq 0.01$; $^{***}p \leq 0.001$; $^{****}p \leq 0.0001$). (D) Copy of Fig. 7C with the number of genes represented by each violin indicated at the bottom. Pairwise two-sided Wilcoxon tests are shown (ns, $p > 0.05$; $^{*}p \leq 0.05$; $^{***}p \leq 0.001$; $^{****}p \leq 0.0001$). (E-F) Copy of Fig. 7D with the number of genes represented by each proportion indicated at the bottom. Pairwise one-sided Fisher's exact tests are shown (ns, $p > 0.05$; $^{*}p \leq 0.05$; $^{***}p \leq 0.001$; $^{****}p \leq 0.0001$). TE, translational efficiency.

References

1. Jiang, X., Cheng, Y., Zhu, Y., Xu, C., Li, Q., Xing, X., Li, W., Zou, J., Meng, L., Azhar, M., et al. (2023). Maternal NAT10 orchestrates oocyte meiotic cell-cycle progression and maturation in mice. Nat Commun 14. 10.1038/s41467-023-39256-0.
2. Liu, Y., Lu, X., Shi, J., Yu, X., Zhang, X., Zhu, K., Yi, Z., Duan, E., and Li, L. (2016). BTG4 is a key regulator for maternal mRNA clearance during mouse early embryogenesis. Journal of Molecular Biology366 8, 366–368.
3. Yu, C., Ji, S.Y., Sha, Q.Q., Dang, Y., Zhou, J.J., Zhang, Y.L., Liu, Y., Wang, Z.W., Hu, B., Sun, Q.Y., et al. (2016). BTG4 is a meiotic cell cycle-coupled maternal-zygotic-transition licensing factor in oocytes. Nat Struct Mol Biol 23, 387–394. 10.1038/nsmb.3204.
4. Martins, J.P.S., Liu, X., Oke, A., Arora, R., Franciosi, F., Viville, S., Laird, D.J., Fung, J.C., and Conti, M. (2016). DAZL and CPEB1 regulate mRNA translation synergistically during oocyte maturation. J Cell Sci, jcs.179218.
5. Sha, Q.Q., Zhu, Y.Z., Li, S., Jiang, Y., Chen, L., Sun, X.H., Shen, L., Ou, X.H., and Fan, H.Y. (2020). Characterization of zygotic genome activation-dependent maternal mRNA clearance in mouse. Nucleic Acids Res 48, 879–894. 10.1093/nar/gkz1111.
6. Zhu, Y., Wu, W., Chen, S., Zhang, Z., Zhang, G., Li, J., and Jiang, M. (2022). Mettl3 downregulation in germinal vesicle oocytes inhibits mRNA decay and the first polar body extrusion during maturation. Biol Reprod 107, 765–778. 10.1093/biolre/ioac112.
7. Rong, Y., Ji, S.Y., Zhu, Y.Z., Wu, Y.W., Shen, L., and Fan, H.Y. (2019). ZAR1 and ZAR2 are required for oocyte meiotic maturation by regulating the maternal transcriptome and mRNA translational activation. Nucleic Acids Res 47, 11387–11402. 10.1093/nar/gkz863.
8. Zhao, L., Zhu, Y., Chen, H., Wu, Y., Pi, S., Chen, L., Shen, L., and Fan, H. (2020). PABPN1L mediates cytoplasmic mRNA decay as a placeholder during the maternal-to-zygotic transition. EMBO Rep 21, 1–15. 10.15252/embr.201949956.
9. Luong, X.G., Daldello, E.M., Rajkovic, G., Yang, C.R., and Conti, M. (2020). Genome-wide analysis reveals a switch in the translational program upon oocyte meiotic resumption. Nucleic Acids Res 48, 3257–3276. 10.1093/nar/gkaa010.
10. Ma, J., Fukuda, Y., and Schultz, R.M. (2015). Mobilization of Dormant Cnot7 mRNA Promotes Deadenylation of Maternal Transcripts During Mouse Oocyte Maturation. Biol Reprod 93, 48. 10.1095/biolreprod.115.130344.
11. Paynton, B. V, Rempel, R., and Bachvarova, R. (1988). Changes in state of adenylation and time course of degradation of maternal mRNAs during oocyte maturation and early embryonic development in the mouse. Dev Biol 129, 304–314. 10.1016/0012-1606(88)90377-6.
12. Chen, J., Melton, C., Suh, N., Oh, J.S.S., Horner, K., Xie, F., Sette, C., Blelloch, R., and Conti, M. (2011). Genome-wide analysis of translation reveals a critical role for deleted in azoospermia-like (Dazl) at the oocyte-to-zygote transition. Genes Dev 25, 755–766. 10.1101/gad.2028911.
13. Takei, N., Sato, K., Takada, Y., Iyyappan, R., Susor, A., and Kotani, T. (2021). Tdrd3 regulates the progression of meiosis II through translational control of Emi2 mRNA in mouse oocytes. Physiology and Genetics, 2021.02.17.431574. 10.1101/2021.02.17.431574.
14. Tay, J., Hodgman, R., and Richter, J.D. (2000). The Control of Cyclin B1 mRNA Translation during Mouse Oocyte Maturation. Dev Biol 221, 1–9.
15. Huarte, J., Belin, D., Vassalli, A., Strickland, S., and Vassalli, J.D. (1987). Meiotic maturation of mouse oocytes triggers the translation and polyadenylation of dormant tissue-type plasminogen activator mRNA. Genes Dev 1, 1201–1211. 10.1101/gad.1.10.1201.
16. Goldman D, Kiessling A, and Cooper G (1988). Post-transcriptional processing suggests that c-mos functions as a maternal message in mouse eggs. Oncogene 3, 159–162.
17. Zhang, B., Zheng, H., Huang, B., Li, W., Xiang, Y., Peng, X., Ming, J., Wu, X., and Zhang, Y. (2016). Allelic reprogramming of the histone modification H3K4me3 in early mammalian development. Nature Publishing Group 537, 553–557. 10.1038/nature19361.